

## Abstract

The Jason-1 satellite, which was launched on December 7, 2001, has been designed to ensure continued observation of the oceans for several decades. The radar altimeter Poseidon-2 emits pulses and measures their round trip time reflected by the ocean. The on-board Jason Microwave Radiometer (JMR), which operates at 18.7, 23.4 and 34 GHz, monitors and corrects the propagation path delays of the altimeter radar signal due to water vapour and non-precipitating liquid water in the atmosphere. In the case of coastal measurements, the JMR field of view (FOV) is already spoiled by the presence of land at 50 kilometres from the coast. Based on the cloud-clearing scheme successfully applied on infrared sounder measurements to remove the cloud contribution, a land-clearing algorithm has been developed for the exploitation of the JMR data in coastal regions. The method uses two or three successive measurements contaminated by consequent proportions of land in order to extract the JMR brightness temperature associated with the sea component of the JMR, taking into account the antenna gain pattern at each frequency. The preliminary tests on simulated database give encouraging results which would make it possible the correction of the JASON altimeter range errors in coastal areas.

## 1- Methodology

The land clearing refers to the process of estimating what the brightness temperature (BT) would be in the absence of land. Here we use an adaptation of the adjacent field-of-view (FOV) approach successfully applied on infrared sounder measurements to remove the cloud contribution.

The observed  $BT_k$  in each coastal FOV  $k$  (first equation in fig 1) is composed by the component  $BT_c$  coming from different types of surfaces, weighted by their corresponding fractional areas  $\alpha_k$ .

For processing optimisation, the problem can be rewritten by introducing the mean pivot  $BT_p$  (mean measure), leading to an alternative formulation (second and third equations in fig 1).

In the adjacent FOV approach, two or more adjacent JMR FOVs are used, where each FOV produces a different realisation of  $BT_k$ , assuming that the different  $BT_c$  are equal but not the  $\alpha_k$  (for each  $j$ ). With these assumptions, the reconstructed ocean BT can be written as a linear combination of the measured BT (Fourth equation in fig 1).

Assuming that the measured BT and the weights are known, the algorithm computes the  $\eta_k$  parameters and the homogeneous  $BT_c$  for ocean and land surfaces.

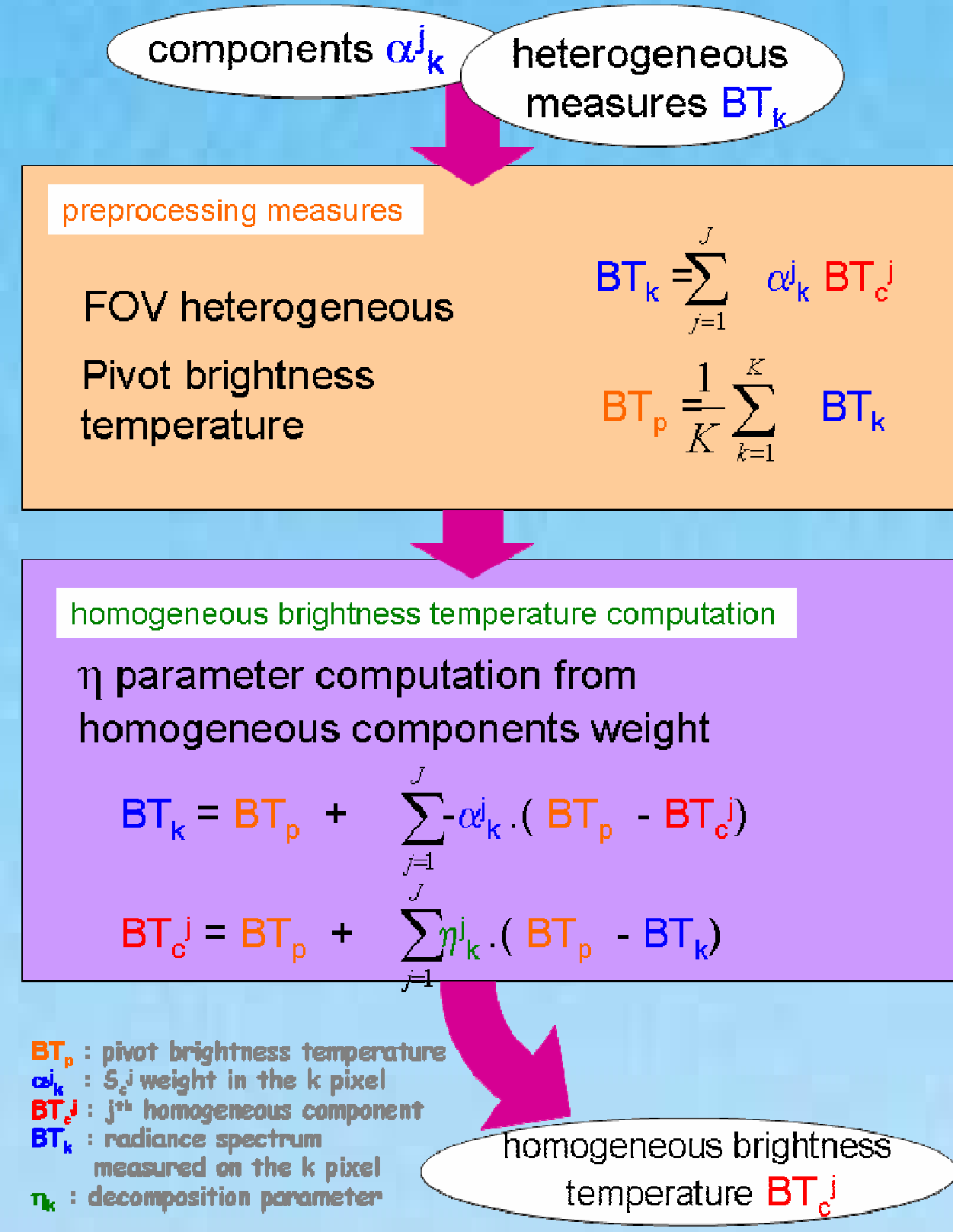


fig. 1: Land-clearing algorithm.

## 4- Land-clearing error source : noise budget

Land-clearing errors have been particularly studied, by considering the two main error sources : the one due to the measurement itself and the second related to the knowledge of the FOV fractional areas  $\alpha_k$ .

The land-cleared BT is a linear combination of the measured BT. This linear combination will have an error standard deviation equal to the standard deviation of the measurement error multiplied by an amplification factor proportional to the root sum square of the weights  $\eta_k$ . This amplification factor is computed by the algorithm in order to quantify the effect of land clearing on the measurement noise.

The  $\alpha_k$  is derived from the coast line position in the FOV. It is obtained from knowledge of the position of the JMR measurement and the precision of the coast mask resolution. It was not evident to take the error on the pixel position and on the geography as a random drawing error or as a bias.

The figure 4 gives an illustration of the land-clearing noise budget as a function of the input measurement error, and with a 1% and 2% error on the component weight in the case of a bias and of a random drawing error.

The amplification coefficient in this case, which was done with an angle of 90° in figure 6 and at 30km from the coast in table 1, is about 3. For 0.8K measurement error, the 2% bias increases the standard deviation of the land-cleared BT of about 0.2K whereas a 2% random error increases the standard deviation of the land-cleared BT of about 0.55 K. Further studies are required in order to simulate properly the error related to fractional area knowledge.

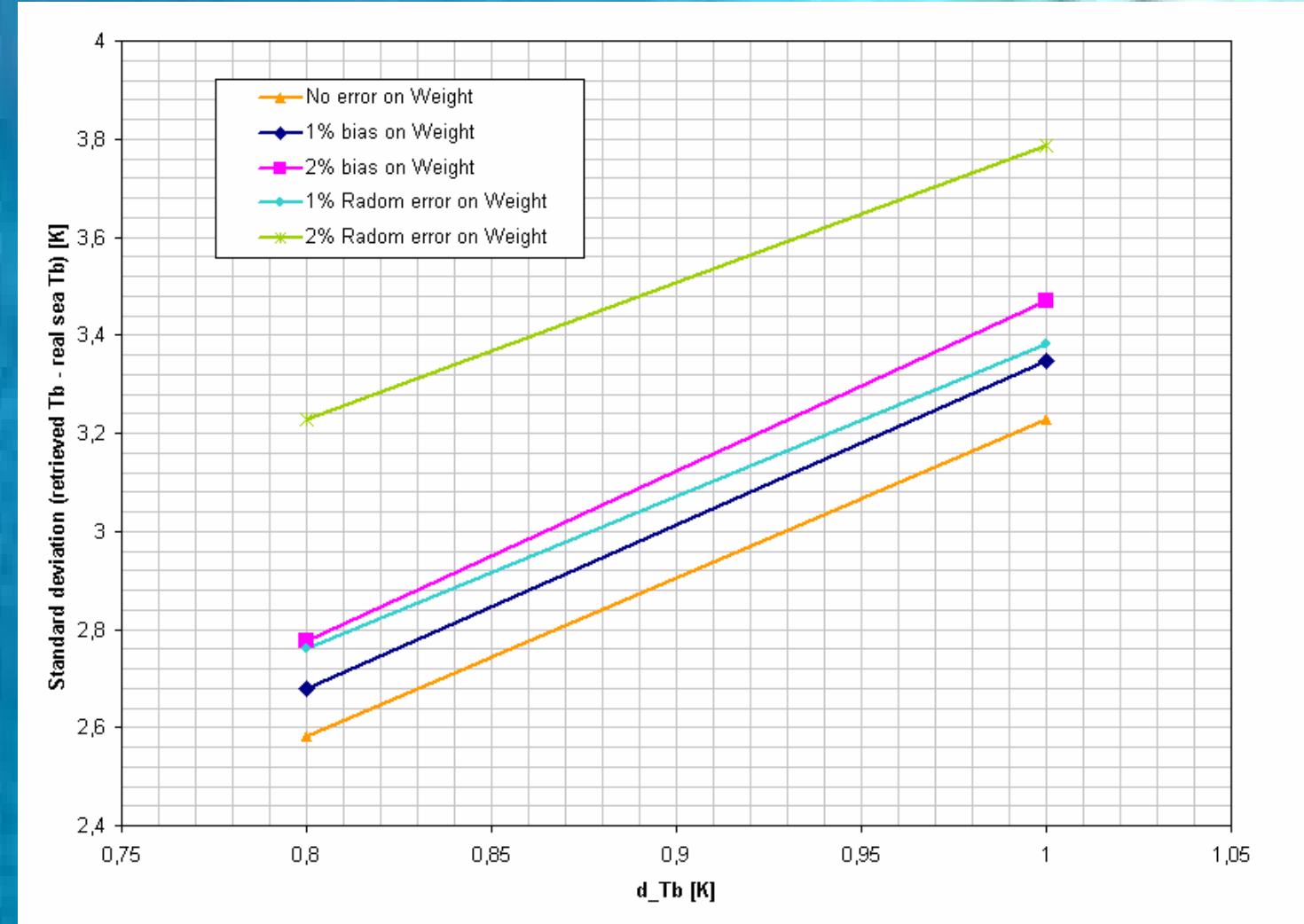


Fig. 4: Comparison between the different manner to consider the error on the weight component.

## 5- Land-clearing error source: Contrast sensitivity

Previous studies [4] showed that the methodology was quite sensitive to the contrast between successive measurements. The contrast studied here comes from the inclination of the satellite's direction related to the coast, which drives the percentage contrast between the three considered adjacent measurements.

The figure 5 displays the standard deviation of the land-cleared brightness temperature as a function of the percentage of sea in the FOVs, for different measurement contrasts. The results presented have been done with a measurement noise of 0.9 K and no error on the component weights. In this case, the gain was not taken into account in input heterogeneous temperature calculation. This shows the strong impact of small contrast percentages on the land-clearing retrieval. Such small contrasts can be found in the case of satellite direction quasi parallel to the coast.

Additional work is required to optimise the algorithm regarding the impact of the measurements contrast on the quality of the retrieved sea component, in particular by exploiting the key role of the Pivots measurement for the management of this effect.

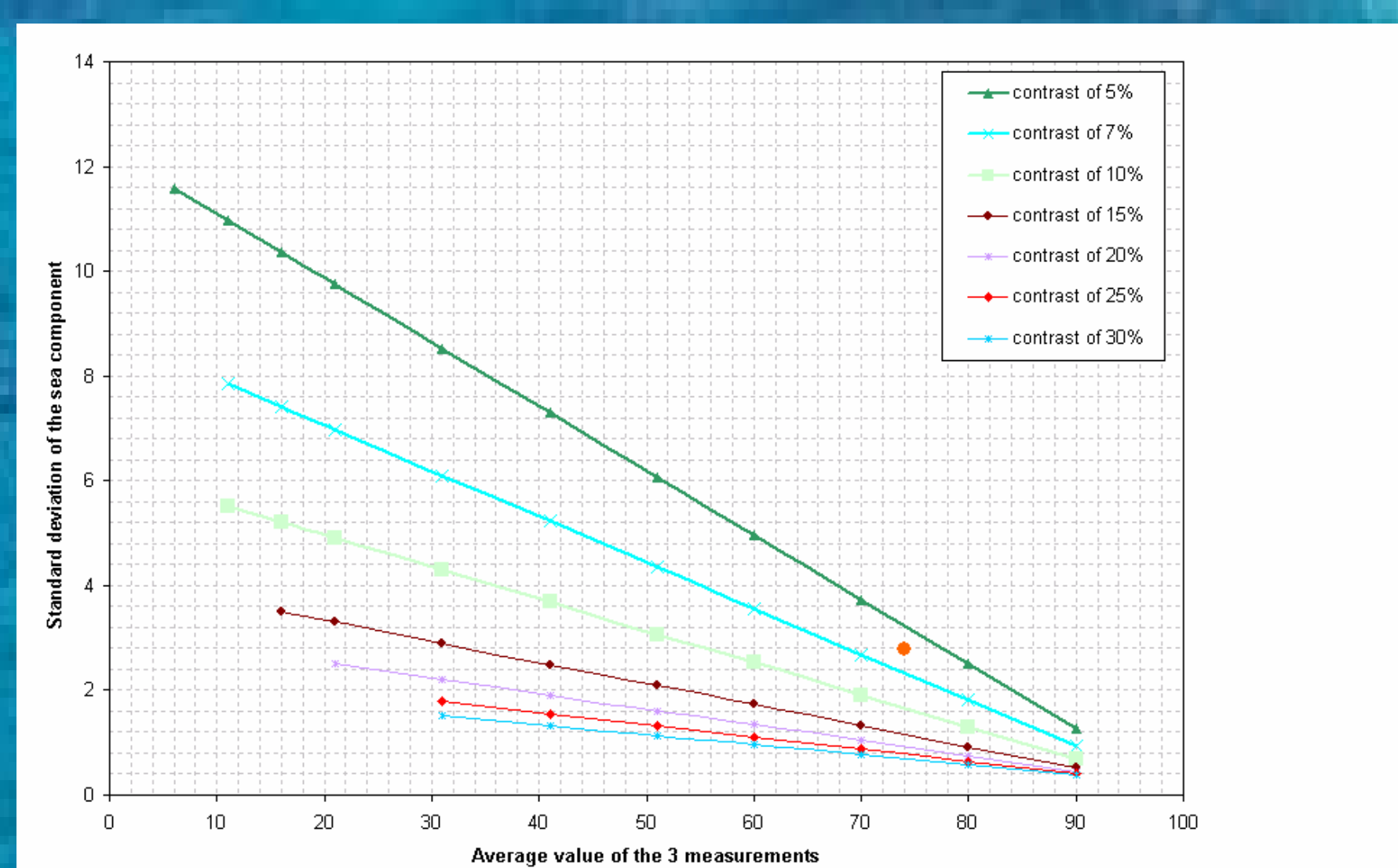


fig. 5: Standard deviation of the land-clearing retrieved brightness temperature of the sea component in different situation of measurement.

## 2- JMR data sets

The Jason Microwave Radiometer collects radiation emitted by the oceans at frequencies 18.7, 23.8 and 34 GHz. Lots of data close to the coast are spoiled by the presence of land.

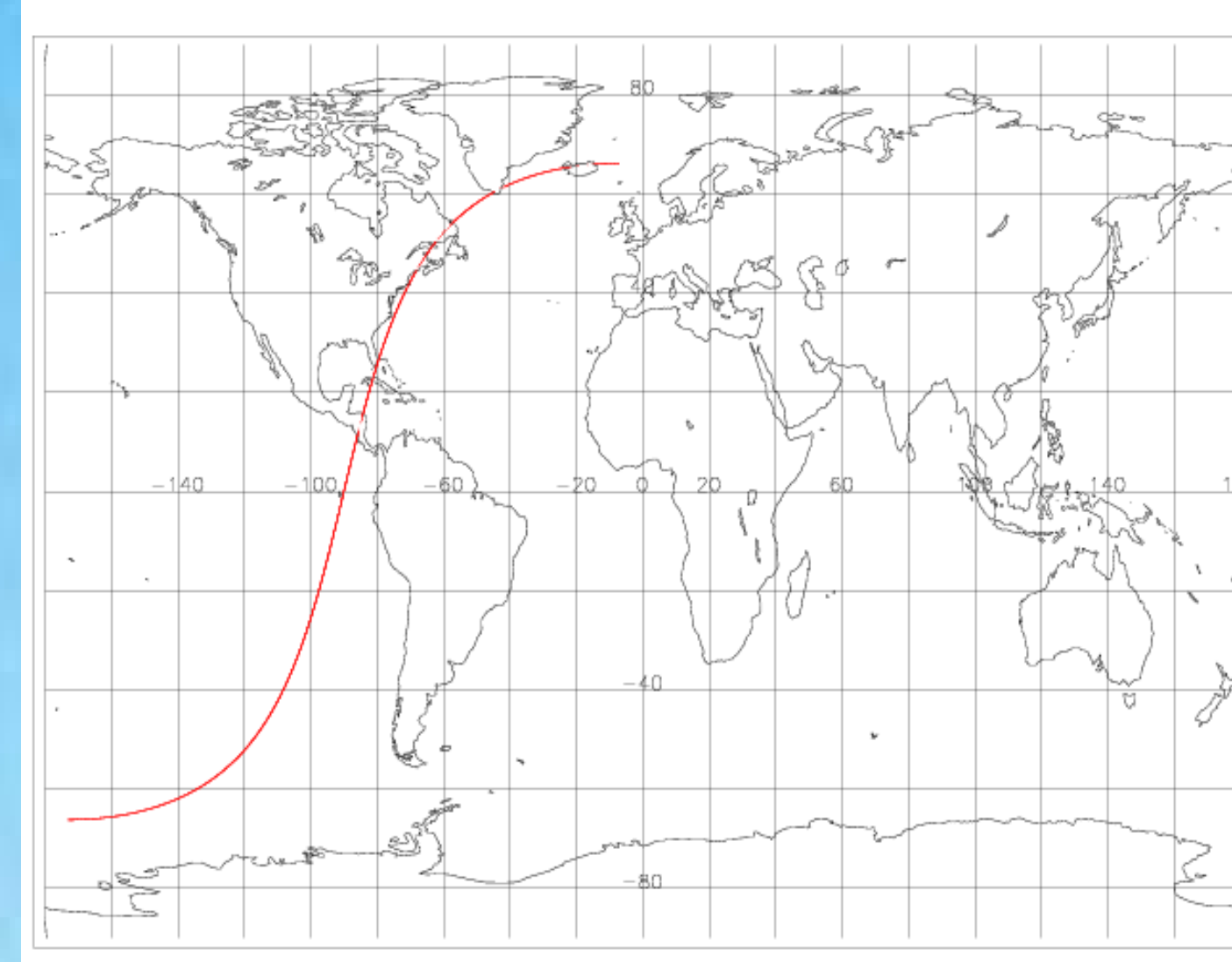


Fig. 2: Pass JA1\_GDR\_2PbP159\_243.

The pass (Fig. 2) gives an example of contaminated data at the three frequencies.

In the mid-latitude, at 34 GHz for example on fig. 3, the brightness temperature can go suddenly from 200K to 290K and back to 180K when the satellite reaches the north

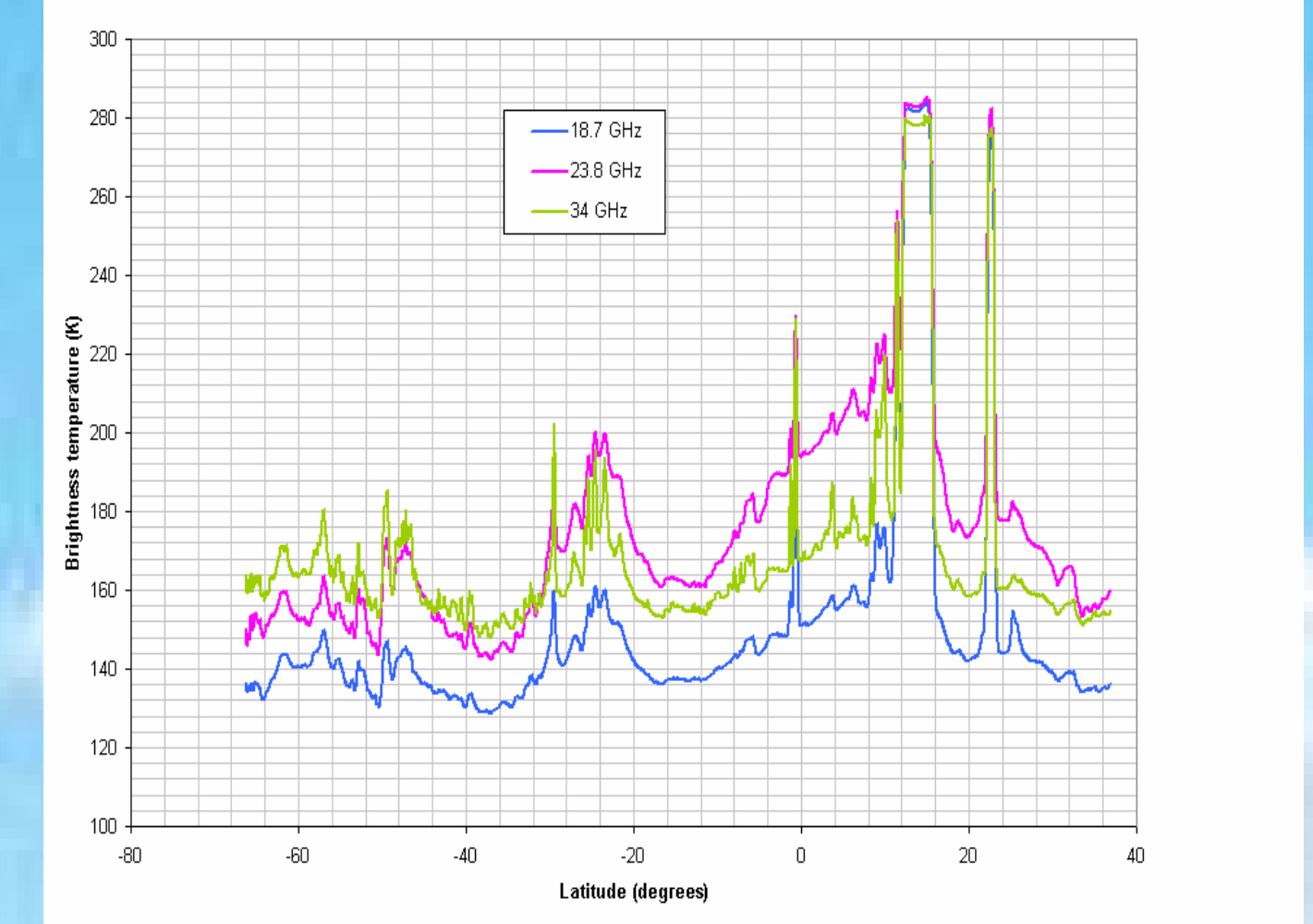


Fig. 3: Brightness temperatures at 18.3, 23.8 and 34 GHz.

of the Canada. The land-clearing method aims to remove land contribution in the radiometer measurements, and improve the estimation of the altimeter path delay correction.

## 3- Simulations cases

The land-clearing algorithm has been tested with simulated antenna brightness temperatures in the case of a presence of coast with a sea component and a land one. The two homogeneous brightness temperatures have been calculated with plane-parallel unpolarized radiative transfer model [1] with a profile chosen within the TIGR 2000 v1.1 [2]. This is a mid-latitude profile with a surface temperature at 280.39 K and a relative humidity of about 85.68%. The surface types are given by the emissivity, which is calculated only over the sea. The land value has been taken from the literature [3].

As the distance from the coast and the BT contrast between adjacent measurements are important (see Fig 5 and associated text), we have tested the land-clearing method with heterogeneous brightness temperatures (taking into account the antenna gain pattern) for the four geographical cases showing in the figure 6, considering angles between satellite direction and coast from 90° at the top to 10° at the bottom of the figure. The first case represents the most contrasted measurements and the contrast decreases with the angle. Three consecutive FOVs are considered. Results compare the error on land-cleared BT with what would be obtained by taking the contaminated (by land) FOV without any processing, supposing a random error of 0.8K on the measurement.

The gain due to the land-clearing is obvious for the 3 first cases. The table 1 shows the improvement of the measured sea brightness temperature in the case of an angle of 90°. In this case, the measurement noise amplification factor due to land clearing processing (see Figure 4 and associated text) is of about 1.3 at 45 km, about 2 at 40 km and about 3 at 30 km. These simulations do not consider the error on the knowledge of ocean and land fractions in the FOVs (see Figure 4 and the associated text).

| Distance from coast | Tb without correction [K] | Tb with land-clear correction [K] |
|---------------------|---------------------------|-----------------------------------|
| 50 km               | 0.79                      | 0.61                              |
| 40 km               | 5.78                      | 1.59                              |
| 30 km               | 11.20                     | 2.58                              |
| 15 km               | 19.60                     | 4.04                              |
| 10 km               | 23.52                     | 4.73                              |
| 5 km                | 24.80                     | 4.96                              |

Table 1: Difference between the measured brightness temperature and the real sea brightness temperature, with (in blue) and without (in pink) the land-clearing correction at an angle of 90° to the coast.

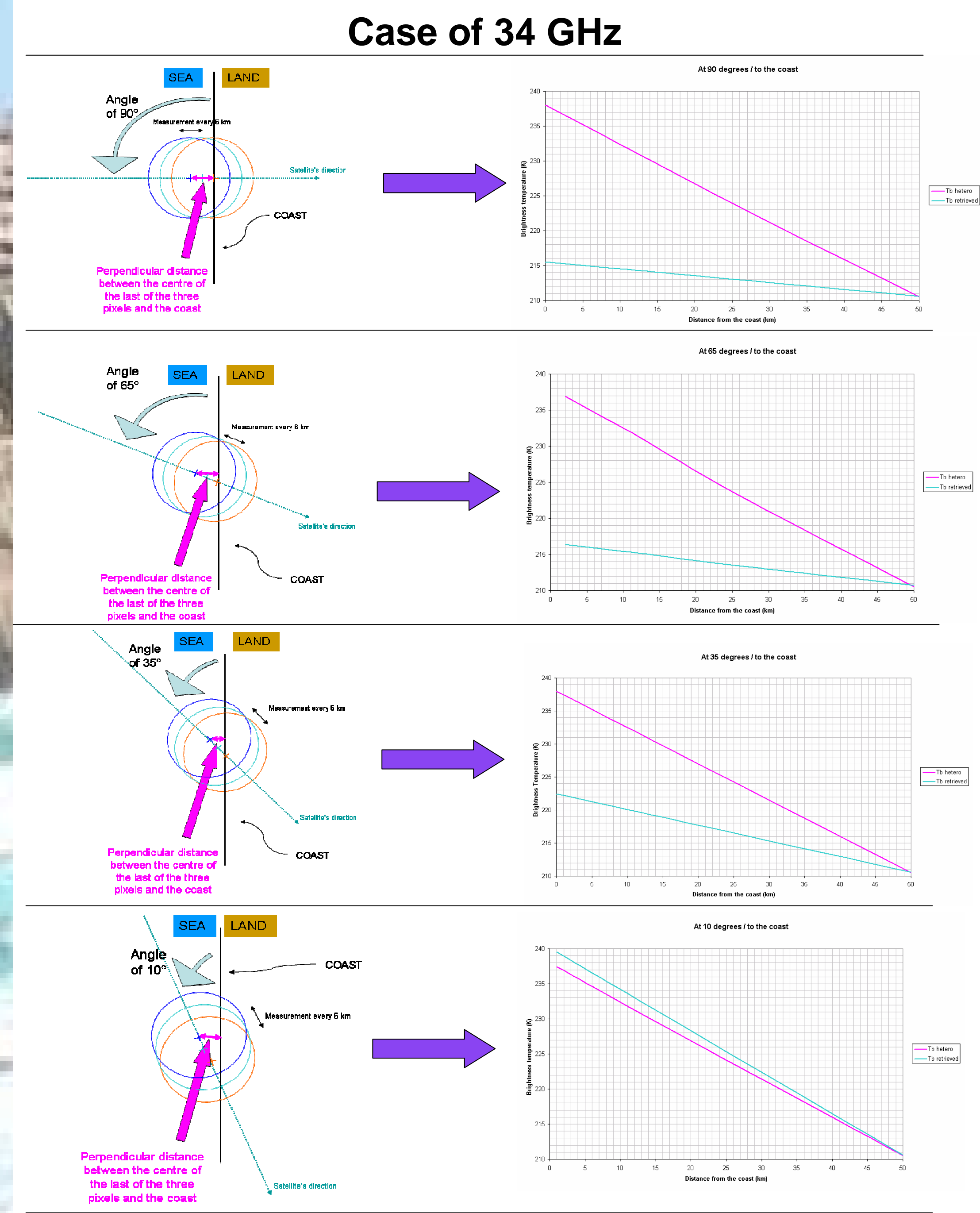


fig. 6: Measured brightness temperature (in pink) and retrieved sea component brightness temperature (in blue) versus the distance of the last measurement from the coast, for 4 inclinations to the coast.

## 6- Conclusion

This preliminary study shows the possibility of improving coastal altimetric data using corrected JMR measurements over the ocean. A land clearing scheme is developed and tested on a simulation case. First results indicate that it is possible to retrieve, at 40 km from the coast for example, the sea component with a small degradation of the input measurement noise (land cleared brightness temperature error std of 1.59 K for a measurement error std of 0.8 K). This shall be compared to the 5.78 K error if no correction is made. As one goes closer to the coast, the precision of the land-cleared brightness temperature degrades, but the magnitude of the correction on the land-contaminated measurement is large. This balance between the land cleared correction impact and land cleared residual error should be discussed in order to derive the best compromise to improve the altimeter path delay correction.

This results have been obtained with the 34 GHz channel in a given simulation case (specific surface and atmospheric conditions), and can not be considered as fully representative of the land-clearing algorithm potential. Indeed, different surface/atmospheric conditions and measurement configurations can modify both the contrast and the noise amplification. Extensive impact study, based on the use of real data, should be performed for the improvement of the algorithm and the analysis of its performances.

## References:

- [1]: "On the accuracy of the Eddington approximation for radiative transfer in the microwave frequencies", *J. Geophys. Res.*, **98**, pp 2757-2765., 1993.
- [2]: Thermodynamic Initial Guess Retrieval: Climatological library of about 2000 representative atmospheric situations from radiosonde reports
- [3]: "A microwave land emissivity model", *J. Geophys. Res.*, **106**, n°D17, pp 20115-20123, 2001.
- [4]: "Traitement des scènes hétérogènes", Study done at Noveltis, NOV-3396-NT-3392, CNES contract 05/CNES/2350. Available at Noveltis or CNES.